

# Pair production in small-angle Bhabha scattering

A. B. Arbuzov and E. A. Kuraev

Joint Institute for Nuclear Research, 141980 Dubna, Russia

N. P. Merenkov

Physical-Technical Institute, 310108 Kharkov, Ukraine

L. Trentadue

Dipartimento di Fisica, Università di Parma, Italy INFN Sezione di Roma II, 00133, Roma, Italy

(Submitted 6 April 1995)

Zh. Éksp. Teor. Fiz. **108**, 1164–1178 (October 1995)

The radiative corrections due to pair production in small-angle high-energy  $e^+e^-$  Bhabha scattering are considered. The corrections due to the production of virtual pairs as well as real soft and hard pairs are calculated analytically. The collinear and semi-collinear kinematical regions of hard pair production are taken into account. The results in the leading and next-to-leading logarithmic approximations yield an accuracy  $\sim 0.1\%$ . Numerical calculations show that the effects of pair production must be taken into account in the precise luminosity determination at LEP. © 1995 American Institute of Physics.

## 1. INTRODUCTION

The electron-positron scattering process (Bhabha process) at small angles was chosen for mobile precise luminosity measurement at LEP I.<sup>1</sup> The measurement technique provides an accuracy of order 0.1%, or even better.<sup>2</sup> Until recently there has been no adequate theoretical calculations of the Bhabha cross-section.<sup>3,4</sup> The radiative corrections (RC) due to the emission of virtual soft and real hard photons and pairs have to be calculated up to the three-loop level. In our previous paper<sup>3</sup> a program of analytical calculations was carried out. The leading contributions  $\propto (\alpha L/\pi)$ ,<sup>1,2,3</sup> as well as the next-to-leading ones  $\propto \alpha/\pi$ ,  $(\alpha/\pi)^2 L$  were calculated explicitly for processes with the emission of photons (here  $L = \ln Q^2/m_e^2$ ,  $Q^2 \sim 1$  (GeV/c)<sup>2</sup> is the square of the momentum transferred,  $\theta$  is the scattering angle). As for pair production processes, the contributions due to the emission of virtual soft and real hard pairs were considered, but the production of real hard pairs was calculated only in collinear kinematics (CK). In this paper we present a systematic study of hard pair emission in semi-collinear kinematics (SCK). We also present the total contribution to the observable Bhabha cross section due to pair production,

$$e^-(p_1) + e^+(p_2) \rightarrow e^-(q_1) + e^+(q_2) + e^-(p_-) + e^+(p_+), \quad (1)$$

which takes the cuts into account in the detection of the scattered electron and positron. We accept the convention<sup>1-3</sup> by which as an event of the Bhabha process is taken to be one in which the angles of the simultaneously registered particles hitting opposite detectors lie in the ranges

$$\begin{aligned} \theta_{\min} < \theta_e < \theta_{\max} = \rho \theta_{\min}, \\ \pi - \rho \theta_{\min} < \theta_e < \pi - \theta_{\min} \end{aligned} \quad (2)$$

( $\theta_{\min} \sim 3^\circ$ ,  $\rho \geq 1$ ) with respect to the beam directions. The second condition is imposed on the energy fractions of the scattered electron and positron:

$$x_e x_{\bar{e}} > x_c, \quad x_{e,\bar{e}} = 2\varepsilon_{e,\bar{e}}/\sqrt{s}, \quad s = 4\varepsilon^2, \quad (3)$$

where  $\varepsilon$  is the energy of the initial electron (or positron) and  $\varepsilon_{e,(\bar{e})}$  is the energy of the scattered electron (positron); here and in what follows the center-of-mass (CM) reference frames is implied.

Our method of calculating the real hard pair production cross-section to within logarithmic accuracy is to separate the contributions of the collinear and semi-collinear kinematical regions.<sup>5,6</sup> In the first one (CK) we suggest that both electron and positron from the created pair go in the narrow cone about the direction of one of the charged particles [the projectile (scattered) electron  $\mathbf{p}_1$  ( $\mathbf{q}_1$ ) or the projectile (scattered) positron  $\mathbf{p}_2$  ( $\mathbf{q}_2$ )]:

$$\begin{aligned} \widehat{\mathbf{p}_+ \mathbf{p}_-} \sim \widehat{\mathbf{p}_- \mathbf{p}_1} \sim \widehat{\mathbf{p}_+ \mathbf{p}_2} < \theta_0 \ll 1, \\ \varepsilon \theta_0 / m \gg 1, \quad \mathbf{p}_i = \mathbf{p}_1, \mathbf{p}_2, \mathbf{q}_1, \mathbf{q}_2. \end{aligned} \quad (4)$$

The contribution of the CK contains terms of order  $(\alpha L/\pi)^2$  and  $(\alpha/\pi)^2 L$ . In the semi-collinear region only one of the conditions (4) on the angles is fulfilled:

$$\begin{aligned} \widehat{\mathbf{p}_+ \mathbf{p}_-} < \theta_0, \quad \widehat{\mathbf{p}_\pm \mathbf{p}_i} > \theta_0; \quad \text{or} \quad \widehat{\mathbf{p}_- \mathbf{p}_1} < \theta_0, \\ \widehat{\mathbf{p}_+ \mathbf{p}_i} > \theta_0; \quad \text{or} \quad \widehat{\mathbf{p}_- \mathbf{p}_i} > \theta_0, \quad \widehat{\mathbf{p}_+ \mathbf{p}_2} < \theta_0. \end{aligned} \quad (5)$$

The contribution of the SCK contains terms of the form

$$\left(\frac{\alpha}{\pi}\right)^2 L \ln \frac{\theta_0}{\theta}, \quad \left(\frac{\alpha}{\pi}\right)^2 L, \quad (6)$$

where  $\theta = \widehat{\mathbf{p}_- \mathbf{q}_1}$  is the scattering angle. The auxiliary parameter  $\theta_0$  drops out in the total sum of the CK and SCK contributions. We systematically omit the terms without large logarithms, which are of order  $(\alpha/\pi)^2 \text{const} \sim 10^{-5}$ .

We restrict ourselves to the case in which an electron-positron pair is created. The effects due to the other pair creation processes ( $\mu^+ \mu^-$ ,  $\pi^+ \pi^-$  etc.) are at least a factor of ten smaller and can be neglected, as will be seen from the numbers obtained. All possible mechanisms for pair creation

(singlet and non-singlet) as well as the identity of the particles in the final state are taken into account. In the case of small-angle Bhabha scattering only a part of the total of 36 tree-type Feynman diagrams are relevant, namely, the scattering diagrams. Besides that we verified that the interference between the amplitudes describing the production of pairs moving in the electron direction and the positron one cancels. This is known as up-down cancellation.

The sum of the contributions due to virtual pair emission (due to the vacuum polarization insertions in the virtual photon Green's function) and of those due to the real soft pair emission does not contain cubic ( $\propto L^3$ ) terms, but depends on the auxiliary parameter  $\Delta = \delta\varepsilon/\varepsilon$  ( $m_e \ll \delta\varepsilon \ll \varepsilon$ , where  $\delta\varepsilon$  is the energy sum of the soft pair components). The  $\Delta$ -dependence disappears in the total sum after the contributions due to real hard pair production are added. Before summing one has to integrate the hard pair contributions over the energy fractions of the pair components, as well as over those of the scattered electron and positron:

$$\Delta = \frac{\delta\varepsilon}{\varepsilon} < x_1 + x_2, \quad x_e < x = 1 - x_1 - x_2 < 1 - \Delta, \quad (7)$$

$$x_1 = \frac{\varepsilon_+}{\varepsilon}, \quad x_2 = \frac{\varepsilon_-}{\varepsilon}, \quad x = \frac{q_1^0}{\varepsilon},$$

where  $\varepsilon_{\pm}$  are the energies of the positron and electron from the created pair. We consider for definiteness the case when the created hard pair moves close to the direction of the initial (or scattered) electron.

The paper is organized as follows: in the second section we consider the emission of a hard pair in the collinear kinematics. The results are very close to those obtained by one of us (N.P.M) in Ref. 6 for the case of pair production in electron-nuclei scattering and applied to the case of small-angle Bhabha scattering in Ref. 4. For completeness we present very briefly the derivation and give the result, correcting some misprints in Ref. 6. In the third section we consider the semi-collinear kinematical regions. The differential cross-section is obtained there and integrated over the angles and energy fractions of the pair components. In the fourth section we give the expression for the RC contribution to the experimental cross-section due to pair production. The results are illustrated numerically in tables and discussed in the Conclusions.

## 2. THE COLLINEAR KINEMATICS

There are four different CK regions: when the created pair goes in the direction of the incident (scattered) electron or positron. We will consider only two of them corresponding to the initial and the final electron directions. For the case of pair emission parallel to the initial electron it is useful to decompose the particle momenta into longitudinal and transverse components:

$$p_+ = x_1 p_1 + \mathbf{p}_+^{\perp}, \quad p_- = x_2 p_1 + \mathbf{p}_-^{\perp}, \quad q_1 = x p_1 + \mathbf{q}_1^{\perp}, \quad (8)$$

$$x = 1 - x_1 - x_2, \quad q_2 \approx p_2, \quad \mathbf{p}_+^{\perp} + \mathbf{p}_-^{\perp} + \mathbf{q}_1^{\perp} = 0,$$

where  $p_i^{\perp}$  are the two-dimensional momenta of the final particles, which are transverse with respect to the initial electron

beam direction. It is convenient to introduce dimensionless quantities for the relevant kinematical invariants:

$$z_i = \left( \frac{\varepsilon \theta_i}{m} \right)^2, \quad z_1 = \left( \frac{p_-^{\perp}}{m} \right)^2,$$

$$z_2 = \left( \frac{p_+^{\perp}}{m} \right)^2, \quad 0 < z_i < \left( \frac{\varepsilon \theta_0}{m} \right)^2 \gg 1,$$

$$A = \frac{(p_+ + p_-)^2}{m^2} = (x_1 x_2)^{-1} [(1-x)^2 + x_1^2 x_2^2 \times (z_1 + z_2 - 2\sqrt{z_1 z_2} \cos \phi)], \quad (9)$$

$$A_1 = \frac{2p_1 p_-}{m^2} = x_2^{-1} [1 + x_2^2 + x_2^2 z_2],$$

$$A_2 = \frac{2p_1 p_+}{m^2} = x_1^{-1} [1 + x_1^2 + x_1^2 z_1],$$

$$C = \frac{(p_1 - p_-)^2}{m^2} = 2 - A_1,$$

$$D = \frac{(p_1 - q_1)^2}{m^2} - 1 = A - A_1 - A_2,$$

where  $\phi$  is the azimuthal angle between the  $(\mathbf{p}_1 \mathbf{p}_+^{\perp})$  and  $(\mathbf{p}_1 \mathbf{p}_-^{\perp})$  planes.

Keeping only the terms which give non-zero contributions to the cross-section in the limit  $\theta_0 \rightarrow 0$  from the sum over spin states of the square of the absolute value of the matrix element, we find that only 8 from the total 36 Feynman diagrams are essential. They are drawn in Fig. 1.

The result has the factorized form (in agreement with the factorization theorem<sup>8</sup>):

$$\sum_{\text{spins}} |M|^2 \Big|_{\mathbf{p}_+ \cdot \mathbf{p}_- \parallel \mathbf{p}_1} = \sum_{\text{spins}} |M_0|^2 2^7 \pi^2 \alpha^2 \frac{I}{m^4}, \quad (10)$$

where one of the multipliers corresponds to the matrix element in the Born approximation (without pair production):

$$\sum_{\text{spins}} |M_0|^2 = 2^7 \pi^2 \alpha^2 \left( \frac{s^4 + t^4 + u^4}{s^2 t^2} \right), \quad (11)$$

$$s = 2p_1 p_2, \quad t = -Q^2 x, \quad u = -s - t,$$

and the quantity  $I$  which stands for the collinear factor coincides with the expression for  $I_a$  obtained in Ref. 6. We write it here in terms of our kinematical variables:

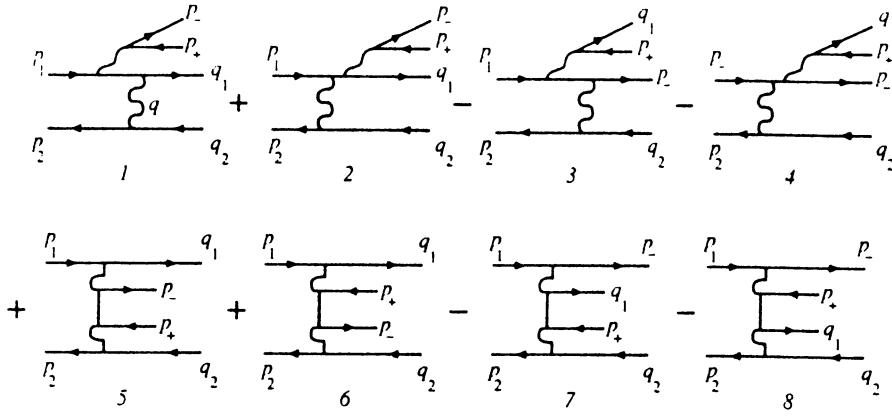


FIG. 1. The Feynman diagrams which give logarithmically reinforced contributions in the kinematical region when the created pair goes in the electron direction. The signs represent the Fermi-Dirac statistics of the interchanged fermions.

$$\begin{aligned}
 I = & (1-x_2)^{-2} \left( \frac{A(1-x_2) + Dx_2}{DC} \right)^2 + (1-x)^{-2} \\
 & \times \left( \frac{C(1-x) - Dx_2}{AD} \right)^2 \\
 & + \frac{1}{2xAD} \left[ \frac{2(1-x_2)^2 - (1-x)^2}{1-x} + \frac{x_1x - x_2}{1-x_2} + 3(x_2 \right. \\
 & \left. - x) \right] + \frac{1}{2xCD} \left[ \frac{(1-x_2)^2 - 2(1-x)^2}{1-x_2} + \frac{x - x_1x_2}{1-x} \right. \\
 & \left. + 3(x_2 - x) \right] + \frac{x_2(x^2 + x_2^2)}{2x(1-x_2)(1-x)AC} + \frac{3x}{D^2} + \frac{2C}{AD^2} \\
 & + \frac{2A}{CD^2} + \frac{2(1-x_2)}{xA^2D} - \frac{4C}{xA^2D^2} - \frac{4A}{D^2C^2} \\
 & + \frac{1}{DC^2} \left[ \frac{(x_1-x)(1+x_2)}{x(1-x_2)} - 2 \frac{1-x}{x} \right]. \quad (12)
 \end{aligned}$$

Rewriting the phase volume of the final particles as

$$\begin{aligned}
 d\Gamma = & \frac{d^3q_1 d^3q_2}{(2\pi)^6 2q_1^0 2q_2^0} (2\pi)^4 \delta^4(p_1x + p_2 - q_1 - q_2) \\
 & \times m^4 2^{-8} \pi^{-4} x_1 x_2 dx_1 dx_2 dz_1 dz_2 \frac{d\phi}{2\pi}, \quad (13)
 \end{aligned}$$

and integrating over the variables of the created pair we obtain (details are presented in the preprint<sup>10</sup>):

$$\begin{aligned}
 \bar{i} = & \int_0^{2\pi} \frac{d\phi}{2\pi} \int_0^{z_0} dz_1 \int_0^{z_0} dz_2 I = \frac{L_0}{2xx_1x_2} \\
 & \times \left\{ D_1 \left( L_0 + 2 \ln \frac{x_1x_2}{x} \right) \right. \\
 & \left. + D_2 \ln \frac{(1-x_2)(1-x)}{xx_2} + D_3 \right\}, \quad L_0 = \ln \left( \frac{\varepsilon\theta_0}{m} \right)^2, \\
 D_1 = & 2xx_1x_2 \left( \frac{1}{(1-x)^4} + \frac{1}{(1-x_2)^4} \right) - \frac{(1-x_2)^2}{(1-x)^2} - \frac{(1-x)^2}{(1-x_2)^2} \\
 & + 1 + \frac{(x+x_2)^2}{2(1-x)(1-x_2)} + \frac{3(x_2-x)^2}{2(1-x)(1-x_2)}
 \end{aligned}$$

$$\begin{aligned}
 & - \frac{x^2 + x_2^2}{(1-x)(1-x_2)} - 2xx_2 \left( \frac{1}{(1-x)^2} + \frac{1}{(1-x_2)^2} \right), \\
 D_2 = & \frac{2(x^2 + x_2^2)}{(1-x)(1-x_2)}, \quad (14) \\
 D_3 = & \frac{2xx_1x_2}{(1-x_2)^2} \\
 & \times \left( -\frac{8}{(1-x_2)^2} + \frac{(1-x)^2}{xx_1x_2} \right) + \frac{2xx_1x_2}{(1-x)^2} \\
 & \times \left[ \frac{x_2}{xx_1} + \frac{2(x_1-x_2)}{xx_1(1-x)} - \frac{8}{(1-x)^2} + \frac{1}{xx_1x_2} - \frac{4}{x(1-x)} \right] \\
 & + 6 + 4x \left[ \frac{x_2 - x_1}{(1-x)^2} - \frac{x_1}{x(1-x)} \right] + \frac{4(xx_2 - x_1)}{(1-x_2)^2} \\
 & - \frac{4(1-x_2)x_1x_2}{(1-x)^3} + \frac{8xx_1x_2^2}{(1-x)^4} - \frac{xx_2^2}{(1-x_2)^4} \\
 & + \frac{x_2}{(1-x_2)^2} \left[ 4(1-x) + \frac{2(x-x_1)(1+x_2)}{1-x_2} \right].
 \end{aligned}$$

Performing similar manipulations in the case when the pair moves in the direction of the scattered electron, integrating the resulting sum over the energy fractions of the pair components, and finally adding the contribution of the two remaining CK regions (when the pair goes in the position directions) we obtain:

$$\begin{aligned}
 d\sigma_{\text{coll}} = & \frac{\alpha^4 dx}{\pi Q_1^2} \int_1^{\rho^2} \frac{dz}{z^2} L \left\{ R_0(x) \left( L + 2 \ln \frac{\lambda^2}{z} \right) (1 + \Theta) \right. \\
 & \left. + 4R_0(x) \ln x + 2\Theta f(x) + 2f_1(x) \right\}, \quad \lambda = \frac{\theta_0}{\theta_{\min}}, \\
 \Theta = & \Theta(x^2\rho^2 - z) = \begin{cases} 1, & x^2\rho^2 > z, \\ 0, & x^2\rho^2 \leq z, \end{cases} \\
 R_0(x) = & \frac{2}{3} \frac{(1+x^2)}{1-x} + \frac{(1-x)}{3x} (4 + 7x + 4x^2) \\
 & + 2(1+x) \ln x, \quad (15)
 \end{aligned}$$

$$f(x) = -\frac{107}{9} + \frac{136}{9}x - \frac{2}{3}x^2 - \frac{4}{3x} - \frac{20}{9(1-x)} + \frac{2}{3} \times \left[ -4x^2 - 5x + 1 + \frac{4}{x(1-x)} \right] \ln(1-x) + \frac{1}{3} \times \left[ 8x^2 + 5x - 7 - \frac{13}{1-x} \right] \ln x - \frac{2}{1-x} \ln^2 \times x + 4(1+x) \ln x \ln(1-x) - \frac{2(3x^2-1)}{1-x} \text{Li}_2(1-x),$$

$$f_1(x) = -x \text{Re} f\left(\frac{1}{x}\right) = -\frac{116}{9} + \frac{127}{9}x + \frac{4}{3}x^2 + \frac{2}{3x} - \frac{20}{9(1-x)} + \frac{2}{3} \left[ -4x^2 - 5x + 1 + \frac{4}{x(1-x)} \right] \times \ln(1-x) + \frac{1}{3} \left[ 8x^2 - 10x - 10 + \frac{5}{1-x} \right] \times \ln x - (1+x) \ln^2 x + 4(1+x) \ln x \ln(1-x) - \frac{2(x^2-3)}{1-x} \text{Li}_2(1-x),$$

$$\text{Li}_2(x) \equiv -\int_0^x \frac{dy}{y} \ln(1-y), \quad Q_1 = \varepsilon \theta_{\min},$$

$$L = \ln \frac{zQ^2}{m^2}.$$

Some misprints, which occur in the expressions for  $f(x)$  and  $f_1(x)$  in Refs. 4, 6, are corrected here.

### 3. THE SEMI-COLLINEAR KINEMATICS

We will restrict ourselves again to the case in which the created pair goes close to the electron momentum (initial or final). A similar treatment applies in the CM system in the case in which the pair follows the positron momentum. There are three different semi-collinear regions, which contribute to the cross-section in the frame to the required accuracy. The first region includes the events for which the created pair has very small invariant mass:

$$4m^2 \ll (p_+ + p_-)^2 \ll |q^2|,$$

and the pair escapes the narrow cones (defined by  $\theta_0$ ) in both the incident and scattered electron momentum directions. We will refer to this SCK region as  $\mathbf{p}_+ \parallel \mathbf{p}_-$ . Only the diagrams 1 and 2 of Fig. 1 contribute in this region; the reason is the smallness (in comparison with  $s$ ) of the square of the four-momentum of the virtual photon converting to the pair.

The second SCK region includes the events for which the invariant mass of the created positron and the scattered electron is small,  $4m^2 \ll (p_+ + q_1)^2 \ll |q^2|$ , with the restriction that the positron should escape the narrow cone in the initial electron momentum direction. We refer to it as  $\mathbf{p}_+ \parallel \mathbf{q}_1$  and note that only the diagrams 3 and 4 of Fig. 1 contribute here.

The third SCK region includes the events in which the created electron goes inside the narrow cone in the initial electron momentum direction but the created positron does not. We refer to it as  $\mathbf{p}_- \parallel \mathbf{p}_1$ . Only the diagrams 7 and 8 of Fig. 1 are relevant there.

The differential cross-section has the following form:

$$d\sigma = \frac{\alpha^4}{8\pi^4 s^2} \frac{|M|^2}{q^4} \frac{dx_1 dx_2 dx}{x_1 x_2 x} d^2 \mathbf{p}_+^\perp d^2 \mathbf{p}_-^\perp d^2 \mathbf{q}_1^\perp d^2 \mathbf{q}_2^\perp \times \delta(1-x_1-x_2-x) \delta^{(2)} \times (\mathbf{p}_+^\perp + \mathbf{p}_-^\perp + \mathbf{q}_1^\perp + \mathbf{q}_2^\perp), \quad |M|^2 = -L_{\lambda\rho} p_{2\lambda} p_{2\rho}, \quad (16)$$

where  $x_1$  ( $x_2$ ),  $x$  and  $\mathbf{p}_+^\perp$  ( $\mathbf{p}_-^\perp$ ),  $\mathbf{q}_1^\perp$  are the energy fractions and the perpendicular momenta of the created positron (electron) and the scattered electron, respectively;  $s = (p_1 + p_2)^2$  and  $q^2 = -Q^2 = (p_2 - q_2)^2 = -\varepsilon^2 \theta^2$  are the center-of-mass energy square and the momentum transferred square; and the leptonic tensor  $L_{\lambda\rho}$  has different forms for different SCK regions.

#### 3.1. The $\mathbf{p}_+ \parallel \mathbf{p}_-$ region

For the region of small  $(p_+ + p_-)^2$  we can use the leptonic tensor obtained in Ref. 6. Keeping only the relevant terms we write it in the form

$$\begin{aligned} \frac{P^4}{8} L_{\lambda\rho} = & \frac{4P^2 q^2}{(1)(2)} \left[ -(p_1 p_1)_{\lambda\rho} - (q_1 q_1)_{\lambda\rho} + (p_1 q_1)_{\lambda\rho} \right. \\ & - 4(p_+ p_-)_{\lambda\rho} \left( 1 - \frac{q^2 P^2}{(1)(2)} \right) - \frac{4}{(1)} [q^2 (p_1 q_1)_{\lambda\rho} \\ & - 2(p_1 p_+) (q_1 p_-)_{\lambda\rho} - 2(p_1 p_-) (q_1 p_1)_{\lambda\rho}] \\ & - \frac{4}{(2)} [P^2 (p_1 q_1)_{\lambda\rho} - 2(p_+ q_1) (p_1 p_-)_{\lambda\rho} \\ & - 2(p_- q_1) (p_1 p_+)_{\lambda\rho}] \\ & - \frac{32(p_1 p_+) (p_1 p_-)}{(1)^2} (q_1 q_1)_{\lambda\rho} \\ & - \frac{32(q_1 p_+) (q_1 p_-)}{(2)^2} (p_1 p_1)_{\lambda\rho} \\ & + \frac{8(p_1 q_1)_{\lambda\rho}}{(1)(2)} [P^2 (p_1 q_1) - 2(p_1 p_+) (p_- q_1) \\ & \left. - 2(p_1 p_-) (q_1 p_+) \right], \quad (17) \end{aligned}$$

where

$$P = p_+ + p_-, \quad (aa)_{\lambda\rho} = a_\lambda a_\rho, \quad (ab)_{\lambda\rho} = a_\lambda b_\rho + a_\rho b_\lambda,$$

$$q = p_1 - q_1 - P, \quad (1) = (p_1 - P)^2 - m^2,$$

$$(2) = (p_1 - q)^2 - m^2.$$

After some algebraic transformations the expression for  $|M|^2$  entering the cross-section can be put in the form

$$\frac{1}{q^4}|M|^2 = -\frac{2s^2}{q^4 p^4} \left\{ -\frac{4P^2 q^2}{(1)(2)} [(1-x_1)^2 + (1-x_2)^2] \right. \\ \left. + \frac{128}{(1)^2(2)^2} [(q_1 p)(p+p_1) - x(p_1 p) \right. \\ \left. \times (q_1 p_+)]^2 \right\}, \quad (18)$$

where  $p = p_- - x_2 p_+ / x_1$ ,  $(\mathbf{q}_2^\perp)^2 = -q^2$ . In this region we can use the relations

$$(1) = -\frac{1-x}{x_1} 2(p_1 p_+), \quad (2) = \frac{1-x}{x_1} 2(q_1 p_+). \quad (19)$$

It is useful to represent all invariants in terms of the Sudakov variables (energy fractions and perpendicular momenta), namely

$$q_1^2 = \frac{1}{x_1 x_2} ((\mathbf{p}^\perp)^2 + m^2(1-x)^2), \\ 2(q_1 p_+) = \frac{1}{x x_1} (x \mathbf{p}_+^\perp - x_1 \mathbf{q}_1^\perp)^2, \\ 2(p_1 p_+) = \frac{1}{x_1} (\mathbf{p}_+^\perp)^2, \quad 2(p_1 p) = \frac{2}{x_1^2} \mathbf{p}_+^\perp \cdot \mathbf{p}_+^\perp, \\ 2(q_1 p) = \frac{2}{x_1^2} (\mathbf{p}_+^\perp [x \mathbf{p}_+^\perp - x_1 \mathbf{q}_1^\perp]), \quad (20)$$

$$\mathbf{p}^\perp = x_1 \mathbf{p}_+^\perp - x_2 \mathbf{p}_+^\perp.$$

A large logarithm appears in the cross-section after the integration over  $\mathbf{p}^\perp$ . In order to carry out this integration we can use the relation

$$\delta^{(2)} d^2 p_+^\perp d^2 p_-^\perp = \frac{1}{(1-x)^2} d^2 \mathbf{p}^\perp, \quad (21)$$

which is valid in the region  $\mathbf{p}_+ \parallel \mathbf{p}_-$ . After the integration we find the contribution of the first SCK region to the cross-section.

$$d\sigma_{\mathbf{p}_+ \parallel \mathbf{p}_-} = \frac{\alpha^4}{\pi} L dx dx_2 \frac{d(\mathbf{q}_2^\perp)^2}{(\mathbf{q}_2^\perp)^2} \frac{d(\mathbf{q}_1^\perp)^2}{(\mathbf{q}_1^\perp + \mathbf{q}_2^\perp)^2} \\ \times \frac{d\phi}{2\pi} \frac{1}{(\mathbf{q}_1^\perp + x \mathbf{q}_2^\perp)^2} \left[ (1-x_1)^2 + (1-x_2)^2 - \frac{4x x_1 x_2}{(1-x)^2} \right], \quad (22)$$

$$\begin{cases} 1 > \cos \phi > -1 + \frac{\lambda^2(1-x)^2 - (\sqrt{z_1} - \sqrt{z_2})^2}{2\sqrt{z_1 z_2}}, & |\sqrt{z_1} - \sqrt{z_2}| < \lambda(1-x), \\ 1 > \cos \phi > -1, & |\sqrt{z_1} - \sqrt{z_2}| > \lambda(1-x), \quad \lambda = \theta_0 / \theta_{\min}, \end{cases} \quad (25)$$

$$\begin{cases} 1 > \cos \phi > -1 + \frac{\lambda^2 x^2 (1-x)^2 - (\sqrt{z_1} - x \sqrt{z_2})^2}{2x \sqrt{z_1 z_2}}, & |\sqrt{z_1} - x \sqrt{z_2}| < \lambda x(1-x), \\ 1 > \cos \phi > -1, & |\sqrt{z_1} - x \sqrt{z_2}| > \lambda x(1-x). \end{cases} \quad (26)$$

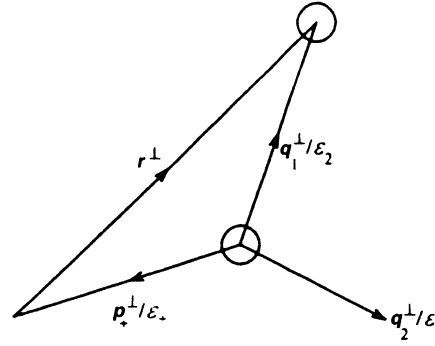


FIG. 2. The kinematics of an event in the angular perpendicular plane corresponding to the SCK region  $\mathbf{p}_+ \parallel \mathbf{p}_-$ .

where  $\phi$  is the angle between the two-dimensional vectors  $\mathbf{q}_1^\perp$  and  $\mathbf{q}_2^\perp$ .

At this stage it is necessary to use the restrictions on the two-dimensional momenta  $\mathbf{q}_1^\perp$  and  $\mathbf{q}_2^\perp$ . They appear when we exclude the contribution of the CK region (which in this case represents the narrow cones with opening angle  $\theta_0$  in the momentum directions of both incident and scattered electrons).

The kinematics of the events corresponding to the region  $\mathbf{p}_+ \parallel \mathbf{p}_-$  in the perpendicular plane is shown in Fig. 2. The circles of radius  $\theta_0$  represent the forbidden collinear regions. Elimination of those regions yields the following restrictions:

$$\left| \frac{\mathbf{p}_+^\perp}{\epsilon_+} \right| > \theta_0, \quad |\mathbf{r}^\perp| = \left| \frac{\mathbf{p}_+^\perp}{\epsilon_+} - \frac{\mathbf{q}_1^\perp}{\epsilon_2} \right| > \theta_0, \quad (23)$$

where  $\epsilon_+$  and  $\epsilon_2$  are the energies of the created positron and the scattered electron, respectively. In order to exclude  $\mathbf{p}_+^\perp$  from the above equation we use the conservation of the perpendicular momentum in the region  $\mathbf{p}_+ \parallel \mathbf{p}_-$ :

$$\mathbf{q}_1^\perp + \mathbf{q}_2^\perp + \frac{1-x}{x_1} \mathbf{p}_+^\perp = 0. \quad (24)$$

It is useful to introduce the dimensionless variables  $z_{1,2} = (\mathbf{q}_{1,2}^\perp)^2 / (\epsilon \theta_{\min})^2$ , where  $\theta_{\min}$  is the minimum angle at which the scattered particles (electron and positron) are recorded by the detector. Here we consider only the symmetrical circular detectors. The conditions (23) can be rewritten as follows

Restriction (26) excludes the phase space corresponding to the narrow cone in the direction of the initial electron, while Eq. (26) excludes that parallel to the scattered electron.

The conditions of the LEP I experiment are

$$\theta_0 \gg \frac{m}{\varepsilon} \approx 10^{-5} \quad \text{and} \quad \theta_{\min} \sim 10^{-2}. \quad (27)$$

This is the reason for considering  $\lambda \ll 1$ . The procedure for integrating the differential cross-section over regions (25) and (26) is described in detail in Ref. 10. Here we give the contribution of the SCK region  $\mathbf{p}_+ \parallel \mathbf{p}_-$  to the cross-section, assuming that only the scattered electrons with energy fraction  $x$  greater than  $x_c$  can be recorded:

$$\begin{aligned} \sigma_{\mathbf{p}_+ \parallel \mathbf{p}_-} &= \frac{\alpha^4}{\pi Q_1^2} \mathcal{L} \int_1^{\rho^2} \frac{dz}{z^2} \int_{x_c}^{1-\Delta} dx \int_0^{1-x} dx_2 \\ &\times \left[ \frac{(1-x_1)^2 + (1-x_2)^2}{(1-x)^2} - \frac{4xx_1x_2}{(1-x)^2} \right] \\ &\times \left\{ (1+\Theta) \ln \frac{z}{\lambda^2} + \Theta \ln \frac{(x^2\rho^2-z)^2}{x^2(x\rho^2-z)^2} \right. \\ &\left. + \ln \left| \frac{(z-x^2)(\rho^2-z)(z-1)}{(z-x^2)^2(z-x^2\rho^2)} \right| \right\}, \quad (28) \end{aligned}$$

$$\mathcal{L} = \ln \frac{\varepsilon^2 \theta_{\min}}{m^2},$$

where  $Q_1^2 = \varepsilon^2 \theta_{\min}^2$ ,  $\rho = \theta_{\max}/\theta_{\min}$  ( $\theta_{\max}$  is the maximum angle of the final particle registration),  $\Theta \equiv \Theta(x^2\rho^2-z)$ ,  $z \equiv z_2$ . The auxiliary parameter  $\Delta$  entering Eq. (28) defines the minimum energy of the created hard pair,  $2m/\varepsilon \ll \Delta \ll 1$ . Note that we replaced  $L$  by  $\mathcal{L}$  because they do not differ at the one-logarithm level.

### 3.2. The $\mathbf{p}_+ \parallel \mathbf{q}_1$ region

As was already mentioned, in the SCK region  $\mathbf{p}_+ \parallel \mathbf{q}_1$  only diagrams 3 and 4 of Fig. 1 contribute. The leptonic tensor in this case can be derived from Eq. (17) by the substitution  $p_- \leftrightarrow q_1$ , and the square of the matrix element can be written as

$$\begin{aligned} |M|_{\mathbf{p}_+ \parallel \mathbf{q}_1}^2 &= -\frac{4s^2}{q_1'^2 q_2^2} \frac{1}{(l')(2)} \left\{ (1-x_1)^2 + (1-x_2)^2 \right. \\ &\left. + \frac{32}{q_1'^2 q_2^2} \frac{1}{(l')(2)} [(p_1 p_+) (p-p') \right. \\ &\left. - x_2 (p-p_+) (p_1 p') \right]^2 \Big\}, \quad (29) \end{aligned}$$

where

$$p' = q_1 - p_+ x/x_1, \quad q_1'^2 = (q_1 + p_+)^2,$$

$$(2) = 2(p_+ p_-)(1-x_2)/x_1,$$

$$(l') = 2(p_1 p_+)(1-x_2)/x_1.$$

The integration of the matrix element over  $(\mathbf{p}_1^\perp)^2$  and  $(\mathbf{p}_-^\perp)^2$  can be carried out analogously to the previous case, and the contribution of the  $\mathbf{p}_+ \parallel \mathbf{q}_1$  region can be represented in the form

$$\begin{aligned} d\sigma_{\mathbf{p}_+ \parallel \mathbf{q}_1} &= \frac{\alpha^4}{\pi} L dx dx_2 \frac{d(\mathbf{q}_2^\perp)^2}{(\mathbf{q}_2^\perp)^2} \frac{d(\mathbf{q}_1^\perp)^2}{(\mathbf{q}_1^\perp)^2} \\ &\times \frac{d\phi}{2\pi} \frac{1}{(\mathbf{q}_1^\perp + x\mathbf{q}_2^\perp)^2} \\ &\times \frac{x^2}{(1-x_2)^2} \left[ \frac{(1-x)^2 + (1-x_1)^2}{(1-x_2)^2} - \frac{4xx_1x_2}{(1-x_2)^2} \right]. \quad (30) \end{aligned}$$

The restriction on the phase space coming from the exclusion of the collinear region when the created pair moves inside the narrow cone in the direction of the scattered electron leads to the relation

$$\left| \frac{\mathbf{p}_-^\perp}{\varepsilon_-} - \frac{\mathbf{q}_1^\perp}{\varepsilon_2} \right| > \theta_0. \quad (31)$$

In Eq. (31) we have to exclude  $\mathbf{p}_-^\perp$  by using conservation of the perpendicular momentum in the case under consideration:

$$\mathbf{p}_-^\perp + \mathbf{q}_2^\perp + \mathbf{q}_1^\perp(1-x_2)/x = 0.$$

In terms of the dimensionless variables  $z_1, z_2$  and the angle  $\phi$ , Eq. (31) can be rewritten as

$$\begin{cases} 1 > \cos \phi > -1 + \frac{\lambda^2 x^2 x_2^2 - (\sqrt{z_1 - x\sqrt{z_2}})^2}{2x\sqrt{z_1 z_2}}, & |\sqrt{z_1 - x\sqrt{z_2}}| < \lambda x x_2, \\ 1 > \cos \phi > -1, & |\sqrt{z_1 - x\sqrt{z_2}}| > \lambda x x_2. \end{cases} \quad (32)$$

The integration of the differential cross-section (30) over the region defined in Eq. (32) leads to the following result for the contribution of the  $\mathbf{p}_+ \parallel \mathbf{q}_1$  SCK region:

$$\begin{aligned} \sigma_{\mathbf{p}_+ \parallel \mathbf{q}_1} &= \frac{\alpha^4}{\pi Q_1^2} \mathcal{L} \int_1^{\rho^2} \frac{dz}{z^2} \int_{x_c}^{1-\Delta} dx \int_0^{1-x} dx_2 \\ &\times \left[ \frac{(1-x)^2 + (1-x_1)^2}{(1-x_2)^2} - \frac{4xx_1x_2}{(1-x_2)^4} \right] \end{aligned}$$

$$\times \left\{ \ln \frac{z}{\lambda^2} + \ln \frac{(\rho^2-z)(z-1)}{x_2^2 \rho^2} \right\}. \quad (33)$$

### 3.3. The $\mathbf{p}_- \parallel \mathbf{p}_1$ region

In the  $\mathbf{p}_- \parallel \mathbf{p}_1$  SCK region only the diagrams 7 and 8 of Fig. 1 contribute to the cross-section to within the required

accuracy. The leptonic tensor in this case can be derived from Eq. (17) by the substitution  $p_1 \leftrightarrow -p_+$ , and the matrix element square has the form

$$|M|_{\mathbf{p}_- \parallel \mathbf{p}_1}^2 = -\frac{4s^2}{q_2'^2 q_2^2} \frac{1}{(I)(2')} \left\{ (1-x)^2 + (1-x_1)^2 + \frac{32}{q_2'^2 q_2^2} \frac{1}{(I)(2')} [x_1(p_1 \tilde{p})(p_1 p_+) + x(p_+ \tilde{p}) \times (q_1 p_1)]^2 \right\}, \quad (34)$$

where

$$\tilde{p} = p_- - x_2 p_1, \quad q_2'^2 = (p_1 - p_-)^2, \\ (2') = -2(p_1 q_1)(1-x_2), \quad (I) = -2(p_1 p_+)(1-x_2). \quad \text{or}$$

$$\left\{ \begin{array}{l} 1 > \cos \phi > -1 + \frac{\lambda^2 x_1^2 - (\sqrt{z_1} - \sqrt{z_2})^2}{2\sqrt{z_1 z_2}}, \quad |\sqrt{z_1} - \sqrt{z_2}| < \lambda x_1, \\ 1 > \cos \phi > -1, \quad |\sqrt{z_1} - \sqrt{z_2}| > \lambda x_1. \end{array} \right. \quad (37)$$

The integration of the differential cross-section (35) over the region defined in Eq. (37) leads to

$$\sigma_{\mathbf{p}_- \parallel \mathbf{p}_1} = \frac{\alpha^4}{\pi Q_1^2} \mathcal{L} \int_1^{\rho^2} \frac{dz}{z^2} \int_{x_c}^{1-\Delta} dx \int_0^{1-x} dx_2 \times \left[ \frac{(1-x)^2 + (1-x_1)^2}{(1-x_2)^2} - \frac{4xx_1x_2}{(1-x_2)^4} \right] \times \left\{ \Theta \ln \frac{z}{\lambda^2} + \Theta \ln \frac{(x^2 \rho^2 - z)^2}{x_1^2 x^4 \rho^4} + \ln \left| \frac{\rho^2(z-x^2)}{z-x^2 \rho^2} \right| \right\}. \quad (38)$$

The total contribution of the semi-collinear kinematics to the cross-section is the sum of Eqs. (28), (33), and (38):

$$\sigma_{s\text{-coll}} = \sigma_{\mathbf{p}_+ \parallel \mathbf{p}_-} + \sigma_{\mathbf{p}_+ \parallel \mathbf{q}_1} + \sigma_{\mathbf{p}_- \parallel \mathbf{p}_1}. \quad (39)$$

#### 4. THE TOTAL CONTRIBUTION DUE TO THE REAL AND VIRTUAL PAIR PRODUCTION

In order to obtain the finite expression for the cross-section we have to add to Eq. (39) the contribution of the collinear kinematics region [Eq. (15)] and those due to the production of virtual and soft pairs. Taking into account the leading and next-to-leading terms we can write the full hard pair contribution as

$$\sigma_{\text{hard}} = \frac{\alpha^4}{\pi Q_1^2} \int_1^{\rho^2} \frac{dz}{z^2} \int_{x_c}^{1-\Delta} dx \left\{ L^2 R(x) + \mathcal{V}[\Theta f(x) + f_1(x)] + \mathcal{V} \int_0^{1-x} dx_2 \left[ \left( \Theta \ln \frac{(x^2 \rho^2 - z)^2}{x^2} + \ln \left| \frac{(z-x^2)(\rho^2-z)(z-1)x^2}{z-x^2 \rho^2} \right| \right) \varphi \right] \right\}$$

The integration of the matrix element over  $(\mathbf{p}_+^\perp)^2$  and  $(\mathbf{p}_-^\perp)^2$  leads to the differential cross-section

$$d\sigma_{\mathbf{p}_- \parallel \mathbf{p}_1} = \frac{\alpha^4}{4\pi} L dx dx_2 \frac{d(\mathbf{q}_2^\perp)^2}{(\mathbf{q}_2^\perp)^2} \frac{d(\mathbf{q}_1^\perp)^2}{(\mathbf{q}_1^\perp)^2} \times \frac{d\phi}{2\pi} \frac{1}{(\mathbf{q}_1^\perp + \mathbf{q}_2^\perp)^2} \left[ \frac{(1-x)^2 + (1-x_1)^2}{(1-x_2)^2} - \frac{4xx_1x_2}{(1-x_2)^4} \right]. \quad (35)$$

The restriction due to the exclusion of the collinear region when the created pair moves inside a narrow cone in the direction of the initial electron has the form

$$\frac{|\mathbf{p}_+^\perp|}{\varepsilon_1} > \theta_0, \quad \mathbf{p}_+^\perp + \mathbf{q}_1^\perp + \mathbf{q}_2^\perp = 0, \quad (36)$$

$$\left. \begin{array}{l} -(\Theta \ln(x\rho^2 - z)^2 + \ln(z-x)^2) \varphi(x, x_2) \\ -(\Theta \ln(x_1^2 x^2 \rho^4) + \ln x_2^2) \varphi(x_2, x) \end{array} \right\}, \quad (40)$$

$$L = \ln \frac{Q_1^2 z}{m^2}, \quad \mathcal{L} = \ln \frac{Q_1^2}{m^2},$$

where

$$\varphi = \varphi(x, x_2) + \varphi(x_2, x),$$

$$\varphi(x_2, x) = \frac{(1-x)^2 + (x+x_2)^2}{(1-x_2)^2} - \frac{4xx_2(1-x-x_2)}{(1-x_2)^4},$$

$$R(x) = \frac{1}{3} \frac{1+x^2}{1-x} + \frac{1-x}{6x} (4+7x+4x^2) + (1+x) \ln x.$$

Integrating over  $x_2$  in the right side of Eq. (40), we obtain the final expression for the cross-section for hard pair production associated with small-angle electron-positron scattering:

$$\sigma_{\text{hard}} = \frac{\alpha^4}{\pi Q_1^2} \int_1^{\rho^2} \frac{dz}{z^2} \int_{x_c}^{1-\Delta} dx \{ L^2 (1 + \Theta) R(x) + \mathcal{V}[\Theta F_1(x) + F_2(x)] \},$$

$$F_1(x) = d(x) + C_1(x), \quad F_2(x) = d(x) + C_2(x),$$

$$d(x) = \frac{1}{1-x} \left( \frac{8}{3} \ln(1-x) - \frac{20}{9} \right),$$

$$C_1(x) = -\frac{113}{9} + \frac{142}{9} x - \frac{2}{3} x^2 - \frac{4}{3x} - \frac{4}{3} (1+x) \times \ln(1-x) + \frac{2}{3} \frac{1+x^2}{1-x} \left[ \ln \frac{(x^2 \rho^2 - z)^2}{(x\rho^2 - z)^2} - 3\text{Li}_2 \right] \quad (41)$$

$$\begin{aligned}
& \times (1-x) \left] + \left( 8x^2 + 3x - 9 - \frac{8}{x} - \frac{7}{1-x} \right) \ln x \right. \\
& \left. + \frac{2(5x^2-6)}{1-x} \ln^2 x + \beta(x) \ln \frac{(x^2\rho^2-z)^2}{\rho^4}, \right. \\
C_2(x) = & -\frac{122}{9} + \frac{133}{9}x + \frac{4}{3}x^2 + \frac{2}{3x} - \frac{4}{3}(1+x) \\
& \times \ln(1-x) + \frac{2}{3} \frac{1+x^2}{1-x} \\
& \times \left[ \ln \left| \frac{(z-x^2)(\rho^2-z)(z-1)}{(x^2\rho^2-z)(z-x)^2} \right| + 3\text{Li}_2(1-x) \right] \\
& + \frac{1}{3} \left( -8x^2 - 32x - 20 + \frac{13}{1-x} + \frac{8}{x} \right) \ln x \\
& + 3(1+x) \ln^2 x \\
& + \beta(x) \ln \left| \frac{(z-x^2)(\rho^2-z)(z-1)}{x^2\rho^2-z} \right|, \\
\beta = & 2R(x) - \frac{2}{3} \frac{1+x^2}{1-x}.
\end{aligned}$$

Formula (41) describes the small-angle high-energy cross-section of the process (1), provided that the created hard pair moves in the direction of the initial electron 3-momentum, and we have now to double  $\sigma_H$  to take into account the production of a hard pair moving in the direction of the initial positron beam.

In order to pick out the dependence on the parameter  $\Delta$  in  $\sigma_H$  we use

$$\begin{aligned}
\int_1^{\rho^2} dz \int_{x_c}^{1-\Delta} dx \Theta(x^2\rho^2-z) &= \int_1^{\rho^2} dz \left[ \int_{x_c}^{1-\Delta} dx - \int_{x_c}^1 dx \bar{\Theta} \right], \\
\bar{\Theta} &= 1 - \Theta(x^2\rho^2-z).
\end{aligned} \tag{42}$$

Hence

$$\int_1^{\rho^2} dz \int_{x_c}^{1-\Delta} \Theta \frac{dx}{1-x} = \int_1^{\rho^2} dz \left[ \ln \frac{1-x_c}{\Delta} - \int_{x_c}^1 \frac{dx}{1-x} \bar{\Theta} \right], \tag{43}$$

$$\begin{aligned}
\int_1^{\rho^2} dz \int_{x_c}^{1-\Delta} dx \Theta \frac{\ln(1-x)}{1-x} &= \int_1^{\rho^2} dz \left[ \frac{1}{2} \ln^2(1-x_c) \right. \\
& - \frac{1}{2} \ln^2 \Delta \\
& \left. - \int_{x_c}^1 dx \frac{\ln(1-x)}{1-x} \bar{\Theta} \right].
\end{aligned} \tag{44}$$

The contribution to the cross-section of the small-angle Bhabha scattering connected with the real soft (with energy less than  $\Delta \cdot \epsilon$ ) and virtual pair production is defined<sup>2</sup> by the formula:

$$\sigma_{\text{soft+virt}} = \frac{4\alpha^4}{\pi Q_1^2} \int_1^{\rho^2} \frac{dz}{z^2} \left\{ L^2 \left( \frac{2}{3} \ln \Delta + \frac{1}{2} \right) \right.$$

TABLE I. The ratio  $S = \sigma_{\text{tot}}/\sigma_0$  in percent, as a function of  $x_c$ , for  $NN$  ( $\rho=1.74$ ,  $\theta_{\text{min}}=1.61$  rad) and  $WW$  ( $\rho=2.10$ ,  $\theta_{\text{min}}=15.0$  rad) counters,  $\sqrt{s} = 2\epsilon = M_Z = 91.187$  GeV.

$x_c$	0.2	0.3	0.4	0.5	0.6	0.7	0.8
$S_{NN}, \%$	-0.018	-0.022	-0.026	-0.029	-0.033	-0.038	-0.046
$S_{WW}, \%$	-0.013	-0.019	-0.024	-0.029	-0.035	-0.042	-0.052

$$+ \mathcal{L} \left( -\frac{17}{6} + \frac{4}{3} \ln^2 \Delta - \frac{20}{9} \ln \Delta - \frac{4}{3} \zeta_2 \right) \}. \tag{45}$$

Using Eqs. (43) and (44) it is easy to check that the auxiliary parameter  $\Delta$  is cancelled in the sum  $\sigma_{\text{tot}} = 2\sigma_{\text{hard}} + \sigma_{\text{soft+virt}}$ , and we can write the total contribution  $\sigma_{\text{tot}}$  as

$$\begin{aligned}
\sigma_{\text{tot}} = & \frac{2\alpha^4}{\pi Q_1^2} \int_1^{\rho^2} \frac{dz}{z^2} \left\{ L^2 \left( 1 + \frac{4}{3} \ln(1-x_c) \right. \right. \\
& \left. \left. - \frac{2}{3} \int_{x_c}^1 \frac{dx}{1-x} \bar{\Theta} \right) + \mathcal{L} \left[ -\frac{17}{3} - \frac{8}{3} \zeta_2 - \frac{40}{9} \right. \right. \\
& \times \ln(1-x_c) + \frac{8}{3} \ln^2(1-x_c) + \int_{x_c}^1 \frac{dx}{1-x} \bar{\Theta} \\
& \times \left( \frac{20}{9} - \frac{8}{3} \ln(1-x) \right) \left. \right] + \int_{x_c}^1 dx [L^2(1 \\
& \left. + \Theta) \bar{R}(x) + \mathcal{L}(\Theta C_1(x) + C_2(x))] \right\}
\end{aligned} \tag{46}$$

$$\bar{R}(x) = R(x) - \frac{2}{3(1-x)}.$$

The right side of Eq. (46) is the master expression for the small-angle Bhabha scattering cross-section connected with the pair production. It is finite and can be used for numerical estimates. Note that the leading term is described by the electron structure function  $D_e^e(x)$ , which represents the probability of finding a positron inside an electron with the four-momentum square up to  $Q^2$ , provided that the electron loses an energy fraction  $(1-x)$ .<sup>9</sup>

In Table I we present the ratio of the RC contribution due to the pair production  $\sigma_{\text{tot}}$  (46) to the normalization cross-section  $\sigma_0$ ,

$$\sigma_0 = \frac{4\pi\alpha^2}{\epsilon^2 \theta_{\text{min}}^2}. \tag{47}$$

In Table II we illustrate the comparison between the non-

TABLE II. Values of  $R_{NN}$  and  $R_{WW}$  as functions of  $x_c$ , where  $R$  represents the ratio of the nonleading contribution in (46) to the total, for  $NN$  and  $WW$  counters.

$x_c$	0.2	0.3	0.4	0.5	0.6	0.7	0.8
$R_{NN}$	0.036	-0.122	-0.194	-0.238	-0.268	-0.335	-0.465
$R_{WW}$	0.179	-0.021	-0.088	-0.120	-0.179	-0.271	-0.415

leading contribution (containing  $\mathcal{L}^1 = \ln Q_1^2/m^2$ ) and the total (containing  $\mathcal{L}^2$  and  $\mathcal{L}^1$ ).

## 5. CONCLUSIONS

Thus, the result derived in this paper combined with the results derived earlier in Refs. 1, 2 give a full and systematic analytical description of the small-angle electron-positron scattering cross-section at LEP I energies accompanied by one- and two-photon radiation and by pair production. The description takes into account the leading and next-to-leading logarithmic approximations and allows the cross-section to be found with the accuracy of better than 0.1%, provided that the scattered electron and positron are recorded by symmetrical circular detectors. With the above derivation it is possible to carry out calculations also for asymmetrical detectors.

Numerical calculations of the virtual and real pair-production RC contributions show that they cancel out at the level of  $10^{-3}$  percent for the given angular apertures and range  $x_c$ . Table II shows that the next-to-leading contribution can be comparable with the leading one. Their ratio is sensitive to  $x_c$  and the range of angles. A similar situation arises for the leading and next-to-leading contributions to the small-angle Bhabha cross-section in the case of the double bremsstrahlung process  $e^- + e^+ \rightarrow e^- + e^+ + \gamma + \gamma$ .<sup>4</sup>

Note that in a realistic case one has to be aware that detectors cannot distinguish a single-particle event from one in which two or more particles hit the same point of the detector simultaneously. In that case the results can easily change: starting from the present differential cross-sections one has to integrate, imposing the needed experimental restrictions.

We want to emphasize also that the method of calculations and many of the results can be used for calculations of

radiative corrections to small- $x$  deep inelastic scattering at HERA. These questions require additional investigations.

We are grateful to V. A. Fadin and L. N. Lipatov for fruitful discussions and criticism. The work was supported in part by INTAS grant 93-1867. One of us (A. B. A.) is thankful to the Royal Swedish Academy of Sciences for the financial support via an ICFPM grant.

<sup>1</sup>B. Pieterzyk, Invited talk at the Radiative Corrections: Status and Outlook Conference, Gatlinburg, TN, USA, 1994, to be published in the Proceedings; preprint LAPP-EXP-94.18.

<sup>2</sup>O. Adriani, M. Aquilar-Benitez *et al.*, Phys. Rep. C **236**, 1 (1993).

<sup>3</sup>S. Jadach, E. Richter-Wąs, Z. Wąs *et al.*, Phys. Lett. B **268**, 253 (1991); Comp. Phys. Commun. **70**, 305 (1992); W. Beenakker and B. Pieterzyk, Phys. Lett. B **296**, 241 (1992); *ibid.* **304**, 687 (1988); D. Bardin, W. Hollik, and T. Riemann, preprints MPI-PAE/Pth 32/90, PHE90-9; M. Böhm, A. Denner, and W. Hollik, Nucl. Phys. B **304**, 687 (1988); W. Beenakker, F. A. Berends and S. C. van der Marck, Nucl. Phys. B **355**, 281 (1991); M. Caffo, H. Czyz, and E. Remiddi, Nuovo Cimento A **105**, 277 (1992).

<sup>4</sup>A. B. Arbuzov, Yad. Fiz. **48**, 1782 (1988); V. S. Fadin, E. A. Kuraev *et al.*, CERN Yellow Report, CERN 95-03, 369 (1995).

<sup>5</sup>N. P. Merenkov, Yad. Fiz. **48**, 1782 (1988) [Sov. J. Nucl. Phys. **48**, 1073 (1988)].

<sup>6</sup>N. P. Merenkov, Yad. Fiz. **50**, 750 (1989) [Sov. J. Nucl. Phys. **50**, 469 (1989)].

<sup>7</sup>V. N. Baier, V. S. Fadin, V. A. Khoze *et al.*, Phys. Rep. C **78**, 293 (1982); V. M. Budnev, I. F. Ginzburg, G. V. Meledin *et al.*, Phys. Rep. C **15**, 183 (1975).

<sup>8</sup>J. C. Collins, D. E. Soper, and G. Sterman, in: *Perturbative QCD*, ed. by A. H. Müller, World Scientific Publ., 1989; V. N. Baier, V. S. Fadin, and V. A. Khoze, Nucl. Phys. B **65**, 381 (1973).

<sup>9</sup>E. A. Kuraev, N. P. Merenkov, and V. S. Fadin, Yad. Fiz. **47**, 1593 (1988) [Sov. J. Nucl. Phys. **47**, 1009 (1988)]; M. Skrzypek, Acta Phys. Polonica B **23**, 135 (1992).

<sup>10</sup>A. B. Arbuzov, E. A. Kuraev, N. P. Merenkov *et al.*, JINR preprint E2-95-110 (1995).

Published in English in the original Russian journal. Reproduced here with stylistic changes by the Translation Editor.